2000

Extended [C I] and (CO)-C-13 (5 -> 4) emission in M17SW

JE Howe

MLN Ashby

EA Bergin

G Chin

NR Erickson
University of Massachusetts - Amherst

See next page for additional authors

Authors

JE Howe, MLN Ashby, EA Bergin, G Chin, NR Erickson, PF Goldsmith, M Harwit, DJ Hollenbach, MJ Kaufman, SC Kleiner, DG Koch, DA Neufeld, BM Patten, R Plume, R Schieder, Ronald L. Snell, JR Stauffer, V Tolls, Z Wang, G Winnewisser, YF Zhang, and GJ Melnick

EXTENDED [C I] AND ^{13}CO(5→4) EMISSION IN M17SW

J. E. Howe[1], M. L. N. Ashby[2], E. A. Bergin[2], G. Chin[3], N. R. Erickson[1], P. F. Goldsmith[4], M. Harwit[5], D. J. Hollenbach[6], M. J. Kaufman[7], S. C. Kleiner[2], D. G. Koch[8], D. A. Neufeld[9], B. M. Patten[2], R. Plume[2], R. Schieder[10], R. L. Snell[1], J. R. Stauffer[2], V. Tolls[2], Z. Wang[2], G. Winnewisser[10], Y. F. Zhang[2], AND G. J. Melnick[2]
Received 2000 May 1; accepted 2000 June 23; published 2000 August 16

ABSTRACT

We mapped a 13×22 pc region in emission from 492 GHz [C I] and, for the first time, 551 GHz ^{13}CO(5→4) in the giant molecular cloud M17SW. The morphologies of the [C I] and ^{13}CO emission are strikingly similar. The extent and intensity of the [C I] and ^{13}CO(5→4) emission is explained as arising from photodissociation regions on the surfaces of embedded molecular clumps. Modeling of the ^{13}CO(5→4) emission in comparison to ^{13}CO(1→0) indicates a temperature gradient across the cloud, peaking to at least 63 K near the M17 ionization front and decreasing to at least 20 K at the western edge of the cloud. We see no correlation between gas density and column density. The beam-averaged column density of C I in the core is 1×10^{18} cm^{-2}, and the mean column density ratio N(C I)/N(CO) is about 0.4. The variations of N(C I)/N(CO) with position in M17SW indicate a similar clump size distribution throughout the cloud.

Subject headings: ISM: individual (M17SW) — ISM: molecules — ISM: structure — radio lines: ISM — submillimeter

1. INTRODUCTION

M17SW is a giant molecular cloud at a distance of 2.2 kpc (Chini et al. 1980) illuminated by the M17 OB association about 1 pc to the east. Studies of molecular excitation (Snell et al. 1984), molecular line profiles (Martin, Sanders, & Hills 1984), and maps of molecular emission (Stutzki & Güsten 1990) from the M17SW core have all concluded that the dense gas is highly clumped. Early photochemical models of molecular cloud/H II region interfaces predicted an overlying layer of ionized carbon and a thin underlying layer of neutral carbon within a photodissociation region (PDR) between the ionized and molecular gas components (e.g., Langer 1976a; Tielens & Hollenbach 1985). Given the edge-on geometry of M17SW and the H II region, observations of [C I] and [C II] emission along cuts through the interface region unexpectedly detected these species more than a parsec into the molecular cloud (Keene et al. 1985; Genzel et al. 1988; Stutzki et al. 1988). Genzel et al. and Stutzki et al. concluded that far-ultraviolet (FUV) radiation penetrates the interclump medium and excites PDRs on the surfaces of illuminated clumps. Subsequent multicomponent PDR models of the cloud have accounted for the intensity of the emission from numerous far-infrared and submillimeter atomic and molecular lines (Burton, Hollenbach, & Tielens 1990; Meixner et al. 1992). Sekimoto et al. (1999) present observations of [C I] emission extending more than a degree southwest of the M17SW cloud core.

The dual radiometers on board the *Submillimeter Wave Astronomy Satellite* (*SWAS*) provide the ability to simultaneously observe the emission from the $J = 5 \rightarrow 4$ rotational transition of ^{13}CO at 550.926 GHz and the $^3P_1 \rightarrow ^3P_0$ fine-structure transition of C I at 492.161 GHz. The roughly $4'$ beamsize of *SWAS* affords us the opportunity to map large regions in the ^{13}CO(5→4) and [C I] lines and study the large-scale physical conditions in and structure of the dense interstellar medium. This is especially important for the ^{13}CO(5→4) line, since few maps are available in the mid-J ^{13}CO transitions beyond the small-scale strip maps of Graf et al. (1993). Whereas the critical density ($n_{cr} \sim 2 \times 10^3$ cm^{-3}) and upper-level energy ($E_u = 24$ K) of [C I] enable it to be easily excited wherever neutral carbon is present in the dense ISM, the ^{13}CO(5→4) line ($n_{cr} \sim 2 \times 10^5$ cm^{-3}; $E_u = 79$ K) will preferentially probe warmer, denser regions.

We obtained with *SWAS* the first large-scale map of the ^{13}CO(5→4) line in M17SW, as well as the [C I] line over the same region. We combine these results with millimeter ^{13}CO observations to probe the physical conditions in the extended cloud and the spatial and density structure of the bulk of the molecular gas.

2. OBSERVATIONS AND RESULTS

We mapped the [C I] and ^{13}CO(5→4) lines in M17SW with *SWAS* between 1999 June 30 and 1999 July 12. We observed a $21' \times 35'$ region (13×22 pc) in mapping mode with a $1'.6$ grid spacing, nodding the telescope between the source position and

[1] Department of Astronomy, University of Massachusetts, Amherst, MA 01003.

[2] Harvard-Smithsonian Center for Astrophysics, 60 Garden Street, Cambridge, MA 02138.

[3] NASA Goddard Spaceflight Center, Greenbelt, MD 20771.

[4] National Astronomy and Ionosphere Center, Department of Astronomy, Cornell University, Space Sciences Building, Ithaca, NY 14853-6801.

[5] 511 H Street SW, Washington, DC 20024-2725; also Cornell University.

[6] NASA Ames Research Center, MS 245-3, Moffett Field, CA 94035.

[7] Department of Physics, San Jose State University, One Washington Square, San Jose, CA 95192-0106.

[8] NASA Ames Research Center, MS 245-6, Moffett Field, CA 94035.

[9] Department of Physics and Astronomy, Johns Hopkins University, 3400 North Charles Street, Baltimore, MD 21218.

[10] I. Physikalisches Institut, Universität zu Köln, Zülpicher Strasse 77, D-50937 Köln, Germany.
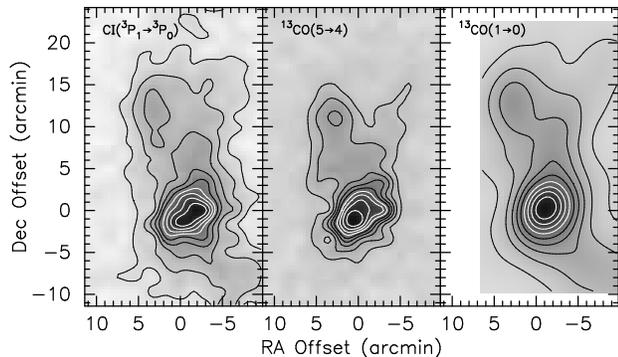
FIG. 1.— Integrated intensity maps of emission from 492 GHz [C I] (*left panel*) and 551 GHz ^{13}CO(5→4) (*center panel*) in M17SW observed by *SWAS*, compared to a ^{13}CO(1→0) map smoothed to equivalent spatial resolution (*right panel*; Wilson et al. 1999). Mapping offsets are relative to position $\alpha = 18^h20^m22\overset{s}{.}1$, $\delta = -16°12'37''$ (J2000). Contour levels for all maps range from 0.1 to 0.9 of the peak in steps of 0.1. Peak intensities (T_A^* scale) are 57.2 K km s^{-1} for [C I], 56.9 K km s^{-1} for ^{13}CO(5→4), and 38.2 K km s^{-1} for ^{13}CO(1→0), integrated over the V_{LSR} range 14–26 km s^{-1}.

a reference position at $\alpha = 18^h25^m13\overset{s}{.}1$, $\delta = -16°50'37''$(J2000). Integration times are typically about 3 minutes, except for 16 central positions observed for H$_2$O detections and described in Snell et al. (2000). The spatial resolution of the observations is about 4′, and the spectral resolution is about 1 km s^{-1}, sampled with a spacing of 0.6 km s^{-1}. The [C I] and ^{13}CO(5→4) linewidths range from about 2–9 km s^{-1} (typically 5 km s^{-1}), so the lines are well resolved. We reduced the spectra using the standard *SWAS* pipeline procedure, and removed small first-order polynomial baseline offsets. Details of the *SWAS* receivers, beam shapes, backend spectrometer, and observing modes are presented in Melnick et al. (2000). We present the maps herein on the T_A^* scale, uncorrected for the *SWAS* main beam efficiency $\eta_{mb} = 0.90$.

We show integrated intensity maps of the [C I] and ^{13}CO(5→4) emission in Figure 1, as well as a ^{13}CO(1→0) map from Wilson, Howe, & Balogh (1999), observed at 47″ resolution with the 14 m telescope of the Five College Radio Astronomy Observatory (FCRAO) but smoothed to 4′.0 resolution for comparison to the *SWAS* observations. The maps include emission within the velocity range (V_{LSR}) 14–26 km s^{-1}, which excludes line-of-sight velocity components not associated with the M17 H II region. The similarity of the morphology and extent of the [C I] and ^{13}CO(1→0) emission is particularly striking. This behavior of the [C I] and low-*J* ^{13}CO emission has also been observed in other giant molecular clouds, notably Orion A (Tauber et al. 1995; Ikeda et al. 1999; Plume et al. 2000), S140 (Plume, Jaffe, & Keene 1994), W3, L1630, and Cep A (Plume et al. 1999). The morphology of the ^{13}CO(5→4) emission is also similar to the [C I] emission but not as extended, except at the eastern edge nearest the H II region. The ^{13}CO(5→4) emission peaks slightly eastward of the [C I] and ^{13}CO(1→0) emission peaks, indicating higher temperatures or gas densities at the eastern edge of the cloud. We explore this further in §3.

The shapes of the [C I] and ^{13}CO lines are quite similar, with the [C I] and ^{13}CO(1→0) line profiles being nearly identical. There are some subtle differences between the ^{13}CO(5→4) line and the other lines, most notably a slight velocity shift at the map center position and slight variances in the red side of the line profile in the northeastern region. Overall, however, the spectra reveal a dynamical as well as morphological similarity between the [C I] and ^{13}CO gas components.
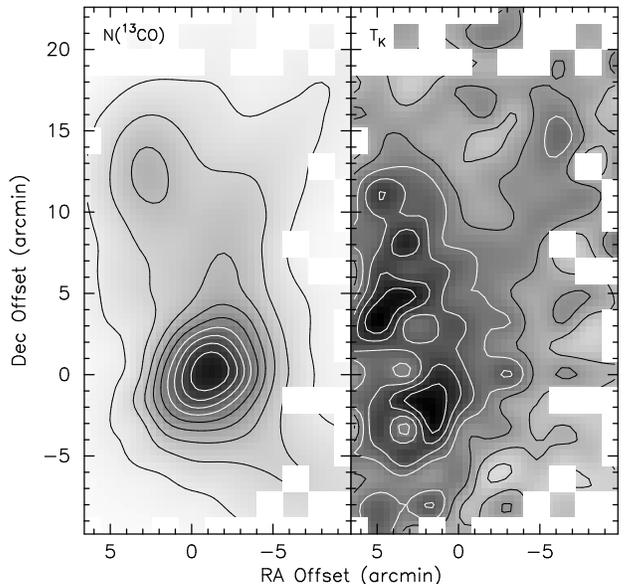

FIG. 2.— Model results for the distribution of ^{13}CO column density (*left panel*) and kinetic temperature (*right panel*) in M17SW. Position offsets are relative to $\alpha = 18^h20^m22\overset{s}{.}1$, $\delta = -16°12'37''$ (J2000). Contour levels range from 0.1 to 0.9 of the peak in steps of 0.1 for $N(^{13}$CO) (peak value 6.1×10^{16} cm^{-2}), and 0.3 to 0.9 of the peak in steps of 0.1 for T_K (peak value 63 K). Regions with ^{13}CO(5→4) detections less than 1σ are blanked.

3. DISCUSSION

3.1. *Temperature, Density, and Column Density Structure*

We used the ^{13}CO(5→4) and ^{13}CO(1→0) integrated intensities together with an iterative algorithm incorporating the Large Velocity Gradient (LVG) radiative transfer approximation (e.g., Scoville & Solomon 1974) to model the ^{13}CO column density $N(^{13}$CO), H$_2$ number density $n(H_2)$, and kinetic temperature T_K. In the LVG modeling we used collision rates for CO with para-H$_2$ (Flower & Launay 1985). Substituting ortho-H$_2$ rates resulted in insignificant differences in the model results. For each position, we began with initial estimates of $T_K = 10$ K, $N(^{13}$CO) appropriate for LTE, and $n(H_2)$ from Snell et al. (1984) for the core or $n(H_2) = 1 \times 10^5$ cm^{-3} elsewhere (Wilson et al. 1999). We used these estimates as input for the LVG algorithm, together with velocity widths derived from the ^{13}CO(1→0) data, to produce model ^{13}CO(5→4) and ^{13}CO(1→0) integrated intensities. We iterated the model with density as the free parameter until the model ^{13}CO(5→4)/^{13}CO(1→0) integrated intensity ratio reproduced the observations. If the $J \leq 5$ level populations thermalized with too low a ratio (i.e. further increases in density no longer affected the line ratio), we incremented T_K and reiterated until the observed ratio was reached. We then iterated the model with $N(^{13}$CO) as the free parameter until the absolute intensities of the lines agreed with observations. This value of $N(^{13}$CO) was then used again in the iteration with $n(H_2)$ to check that line opacity effects did not change the line ratio, and the entire loop repeated as necessary until the model line intensities and ratios agreed with the observations. This procedure then yields the minimum temperatures necessary to explain the line ratios.

The model results show clear evidence that the molecular cloud is heated by the H II region/ionization front at its eastern edge. In Figure 2 we show the temperature distribution over the region mapped in ^{13}CO(1→0) as well as the derived ^{13}CO column density distribution. The peak beam-averaged column density is 6.1×10^{16} cm^{-2}, with a mean value of 1.2×10^{16}

We derive molecular gas densities in the range 1–6×10^5 cm^{-3} over the entire region mapped, with a median value of 3×10^5 cm^{-3}, about half as large as densities derived from multi-transition CS observations of the core region of M17SW (Snell et al. 1984; Wang et al. 1993). In contrast to the well-ordered column density and temperature distribution across the M17SW cloud, the density distribution appears almost random. In particular, there is no correlation between the gas density and the column density. Instead, high- and low-density regions are peppered randomly throughout the region. Since the excitation of the ^{13}CO($5 \rightarrow 4$) emission depends both on the temperature and density, with higher densities requiring lower temperatures for the same $J = 5$ fractional population, we investigated whether there was any trend between T_K and $n(H_2)$ as an artifact of the modeling algorithm. We see no correlation between the gas temperature distribution and the density distribution in the model results.

Although the model distributions of temperature and density are uncorrelated, the densities we derive are sensitive to the model cloud temperature. For example, uniform cloud temperatures of 50 K and 100 K yield median cloud densities of 4×10^4 and 1×10^4 cm^{-3}, respectively. The model column densities are insensitive to temperature, decreasing by only 20 percent if $T_K = 100$ K. Since such large column densities of hot gas are difficult to produce throughout the cloud, and since our model mean cloud temperature is already somewhat higher than the Wilson et al. (1999) global cloud temperature, we consider 4×10^4 cm^{-3} as a reasonable lower limit to the mean cloud density.

The modeling results for the density and column density of the molecular gas in M17SW require that the gas is highly clumped. We derive the volume filling factor of the gas by dividing the ratio of the peak H_2 column density (4×10^{22} cm^{-2}, assuming a ^{13}CO abundance of 1.5×10^{-6} relative to H_2) to the mean H_2 number density (3×10^5 cm^{-3}) by the linear extent of the core (3 pc core size, deconvolved from the *SWAS* beam). From these quantities, we derive a volume filling factor of 0.02. Stutzki & Güsten (1990) derive toward the central $13''$ of the core a volume filling factor of 0.13 for gas with densities greater than 10^5 cm^{-3}, reflecting a higher concentration of clumps at the core peak region.

3.2. *The Correlation of* [C I] *and* ^{13}CO *Emission*

The large extent of the [C I] emission in M17SW and its similarity to isotopic CO emission was first noted by Keene et al. (1985) and Genzel et al. (1988) along linear cuts through the ionization front/molecular cloud interface. The large-scale [C I] and ^{13}CO maps in Figure 1 show that this similarity extends over the entire region mapped. We plot in the top panel of Figure 3 the observed correlation of the integrated intensities of the [C I] and ^{13}CO($1 \rightarrow 0$) emission. We converted the data to the main-beam temperature scale T_{mb} to remove differences in telescope beam efficiencies from the observed relation ($\eta_{mb} = 0.52$ for the FCRAO data; Wilson et al. 1999). The observed trend is well fit (linear least-squares, correlation coefficient 0.95) by the relation $\int T_{mb} dV([\text{C I}]) = (0.84 \pm 0.02) \int T_{mb} dV(^{13}\text{CO}(1 \rightarrow 0)) - (0.4 \pm 0.4)$. The slope of this relation is similar to the slope observed between [C I] and ^{13}CO($2 \rightarrow 1$) in the Orion Bar region by Tauber et al. (1995; ~ 0.8), but is somewhat higher than the relation reported by Ikeda et al. (1999; ~ 0.5) for the Orion A cloud as a whole, and for the ensemble of clouds W3, L1630, S140, and Cep A (Plume et al. 1999). We propose a possible
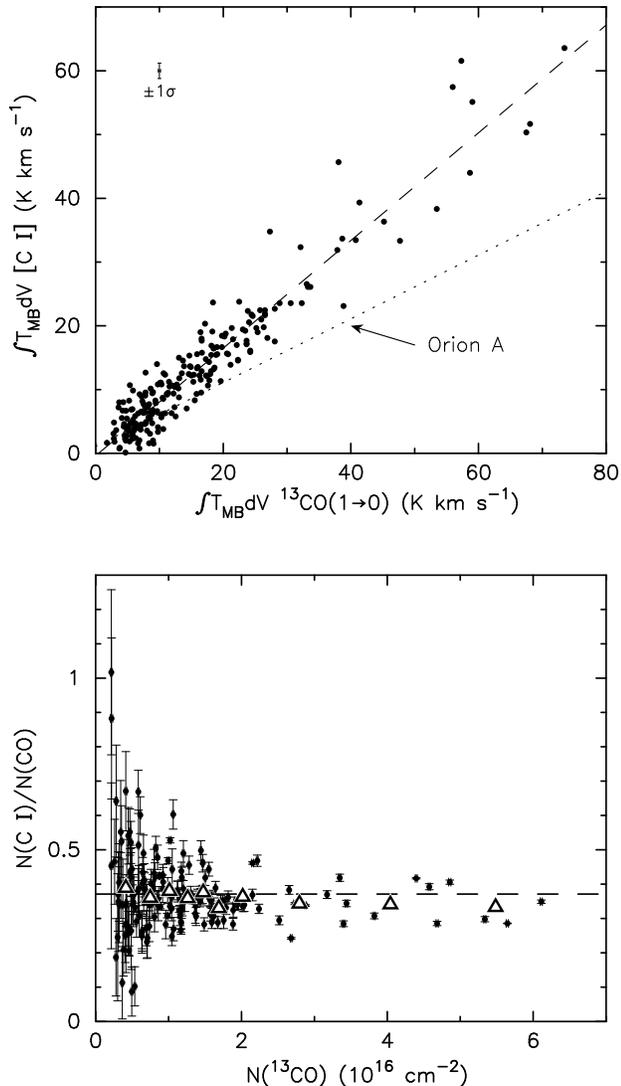
FIG. 3.— (*Top*) The linear correlation of the integrated intensity (T_{MB} scale) of [C I] with ^{13}CO($1 \rightarrow 0$) at each position in M17SW. The dashed line traces the least-squares linear fit to the data (slope 0.84). The dotted line plots the equivalent fit for the Orion A cloud (slope 0.5; Ikeda et al. 1999). (*Bottom*) The derived ratio of the column densities of C I to CO [where $N(\text{CO}) \equiv 50N(^{13}\text{CO})$] is plotted against the ^{13}CO column density at each position in M17SW. Errorbars are $\pm\ 1\sigma$ as described in the text. The dashed line marks the mean value of $N(\text{C I})/N(\text{CO})$ (0.37) for all data points. The triangles plot the value of $N(\text{C I})/N(\text{CO})$ in bins containing equal numbers of ^{13}CO molecules, with the abscissa at the center of each binning range.

cm^{-2}. The column density map appears virtually identical to the ^{13}CO($1 \rightarrow 0$) integrated intensity map (Fig. 1), a property attributable to the low opacity of the ^{13}CO lines ($\tau \lesssim 0.6$ for either line). The highest gas temperatures are found along the eastern edge of the cloud, peaking at about 60 K near the cloud core. The mean cloud temperature is 35 K, similar to the global cloud temperature of 30 K derived by Wilson et al. (1999). The temperature we derive for the core region is also consistent with the temperatures derived from millimeter observations of optically thin CH$_3$CCH emission (Bergin et al. 1994). Our observations apparently are insensitive to the high temperature gas ($T_K \geq 200$ K) responsible for CO($7 \rightarrow 6$) line emission observed in the H II/H$_2$ interface region, however this gas is estimated to comprise only about 5 percent of the total column density (Harris et al. 1987) and would contribute only about 10 percent of the observed peak ^{13}CO($5 \rightarrow 4$) intensity.

explanation for this in §3.3.

We used the *SWAS* [C I] observations to model the C I column density N(C I) in a manner similar to the ^{13}CO LVG modeling, using the collision rates of Schröder et al. (1991). Since the spatial distribution and velocity profiles of the C I and ^{13}CO lines are nearly identical, we used the temperatures and densities derived from the ^{13}CO observations, along with the ^{13}CO(1→0) linewidths, as fixed input parameters to the LVG algorithm. We then iterated the models with N(C I) as the sole free parameter until the model [C I] intensities matched the observations. N(C I) ranges from 1.1×10^{16} cm^{-2} to 1.1×10^{18} cm^{-2} with a median value of 1.7×10^{17} cm^{-2}. The [C I] line is optically thin, with a maximum opacity less than 0.6 at the core. Our peak value of N(C I) is about half that obtained by Sekimoto et al. (1999) in a 2′ beam. The spatial distribution of N(C I) is nearly identical to the distribution of N(^{13}CO) shown in Figure 2.

The derived C I column densities show an interesting behavior when compared to the ^{13}CO column densities. In the bottom panel of Figure 3 we plot the ratio of N(C I) to the CO column density N(CO) (calculated assuming a CO/^{13}CO abundance ratio of 50) as a function of ^{13}CO column density for each model position. Errorbars reflect the random errors of the [C I] and ^{13}CO(1→0) intensities, but not systematic uncertainties in the LVG models. Whereas at the low column densities at the edges of the molecular cloud the N(C I)/N(CO) ratio ranges from 0.1 to 1.0, at high column densities in the core of the cloud the lower and upper bound for the range asymptotically approach the mean N(C I)/N(CO) ratio for all positions (0.37). This is similar to the behavior exhibited for the Orion A cloud, except the mean column density ratio is much lower, only about 0.10 in the Orion core regions (Plume et al. 2000). The behavior of the N(C I)/N(CO) ratio is difficult to understand in the context of chemical models where the neutral carbon is produced *in situ* in the molecular gas (e.g., Langer 1976b; Pineau des Forêts, Roueff, & Flower 1992), and would thereby predict a more or less constant column density ratio. Likewise, simple plane parallel PDR models (e.g., Langer 1976a; Tielens & Hollenbach 1985; Hollenbach, Takahashi, & Tielens 1991) predict a rising value of N(C I)/N(CO) with decreasing molecular gas column density, but not the increased scatter we observe in the ratios. Remarkably, summing the N(^{13}CO)-ordered data of Figure 3 into bins of equal total number of ^{13}CO molecules (in this case, 2×10^{17} cm$^{-2} \times A_{\mathrm{beam}}$, where A_{beam} is the area subtended by the *SWAS* beam at the distance of M17SW), and then computing N(C I)/N(CO) for the binned data, shows that N(C I)/N(CO) is independent of the mean ^{13}CO column density for each bin (see Fig. 3). The resolution to the behavior of N(C I)/N(CO) lies in the structure of the M17SW molecular cloud.

3.3. *PDR Emission and the Structure of M17SW*

Theoretical models of PDRs are quite successful at predicting the observed ^{13}CO(5→4) and [C I] line intensities and the column density of C I for the physical conditions in the region mapped by *SWAS*. Based on the arguments of Stutzki et al. (1988) and Meixner et al. (1992), we expect the incident FUV field within the cloud to range from $\sim 10\ G_0$ at the northwestern edge to $4 \times 10^4\ G_0$ at the ionization front located about 1′5 northeast of the map reference position, where G_0 is in units of the Habing flux. Our LVG modeling indicates a fairly narrow range of densities, 1–6×10^5 cm^{-3}. PDR models predict

a column density N(C I) $\sim 4 \times 10^{17}$ cm^{-2} insensitive to variations in G_0 and only weakly dependent on density (Tielens & Hollenbach 1985). This is similar to the mean value of N(C I) derived for the M17SW cloud. For the peak N(C I) we derive, only a few PDRs along the line of site through the core are required. Kaufman et al. (1999) present updated homogeneous PDR models covering the range of densities and FUV fluxes appropriate for M17SW, and have recently incorporated ^{13}CO into the models for comparison with *SWAS* observations. These models successfully predict the same range of ^{13}CO(5→4) integrated intensities, for the densities and FUV fluxes we find in M17SW, as those observed by *SWAS*. The PDR models of Köster et al. (1994) also predict the peak ^{13}CO(5→4) line temperature we observe, for $G_0 = 10^4$ and n(H$_2$) $= 10^5$ cm^{-3}. The Kaufman et al. (1999) models match the observed [C I] integrated intensities for regions of the cloud with $G_0 < 100$, but are a factor of about 3–4 too low for the core of the cloud. Again, this is easily explained by requiring several PDRs along the line of sight through the core.

The extent of the [C I] emission and the relationship of N(C I) with the molecular gas column density require not only that the gas is clumpy, but that the distribution of clump sizes is similar throughout the cloud, from the core out to the periphery. In a clumpy cloud penetrated by FUV radiation, PDRs arise on the surfaces of the dense clumps, with a thin shell of C I encompassing the CO in the clump. Consider unresolved clumps of similar density, as is the case for the *SWAS* observations (see Stutzki & Güsten 1990). The beam-averaged column density N(C I) depends on the clump surface area while N(CO) depends on the volume, so the ratio N(C I)/N(CO) varies as the inverse size of the clumps. Thus, one might expect for a cloud with a range of clump sizes a large scatter in the column density ratio, as we see in the low column density regions where only a few clumps are probably subtended by the *SWAS* beam. As the beam samples larger column densities, i.e. more clumps in the beam, the clump size distribution is more completely sampled and the scatter in N(C I)/N(CO) decreases, approaching the value appropriate for the mean surface area to volume ratio of the clump size distribution. By summing up the low column density regions we increase the clump sample size, and we see from Figure 3 that the N(C I)/N(CO) ratio for equal total gas masses gives the same value of N(C I)/N(CO). Thus, the size distribution of clumps must be the same throughout the cloud. The diameter of a spherical clump with a C I/CO number ratio of 0.37 and H$_2$ density 3×10^5 cm^{-3} is 0.04 pc, where we assume all carbon is either in C I or in CO and calculate the thickness of the C I layer from Hollenbach et al. (1991). This diameter scales inversely with the H$_2$ density. The lower N(C I)/N(CO) ratio found in Orion is probably a consequence of a larger mean clump size, since N(C I) is insensitive to changes in density and FUV flux. Since the intensity of optically thin lines scales directly with column density, observationally a lower N(C I)/N(CO) ratio produces a lower slope in the linear correlation of the [C I] line intensity to the ^{13}CO(1→0) intensity (e.g, Fig. 3).

REFERENCES

Bergin, E. A., Goldsmith, P. F., Snell, R. L., & Ungerechts, H. 1994, ApJ, 431, 674
Burton, M. G., Hollenbach, D. J., & Tielens, A. G. G. M. 1990, ApJ, 365, 620
Chini, R., Elsässer, H., & Neckel, T. 1980, A&A, 91, 186
Flower, D. R., & Launay, J. M. 1985, MNRAS, 214, 271
Genzel, R., Harris, A. I., Jaffe, D. T., & Stutzki, J. 1988, ApJ, 332, 1049
Graf, U. U., Eckart, A., Genzel, R., Harris, A. I., Poglitsch, A., Russell, A. P. G., & Stutzki, J. 1993, ApJ, 405, 249
Harris, A. I., Stutzki, J., Genzel, R., Lugten, J. B., Stacey, G. J., & Jaffe, D. T. 1987, ApJ, 322, L49
Hollenbach, D., Takahashi, T., & Tielens, A. G. G. M. 1991, ApJ, 377, 192
Ikeda, M., et al. 1999, ApJ, 527, L59
Kaufman, M. J., Wolfire, M. G., Hollenbach, D. J., & Luhman, M. L. 1999, ApJ, 527, 795
Keene, J., Blake, G. A., Phillips, T. G., Huggins, P. J., & Beichman, C. A. 1985, ApJ, 299, 967
Köster, B., Störzer, H., Stutzki, J., & Sternberg, A. 1994, A&A, 284, 545
Langer, W. 1976a, ApJ, 206, 699
Langer, W. 1976b, ApJ, 210, 328
Martin, H. M., Sanders, D. B., & Hills, R. E. 1984, MNRAS, 208, 35
Meixner, M., Haas, M. R., Tielens, A. G. G. M., Erickson, E. F., & Werner, M. 1992, ApJ, 390, 499
Melnick, G. J., et al. 2000, ApJ, 539, L77

Pineau des Forêts, G., Roueff, E., & Flower, D. R. 1992, MNRAS, 258, 45
Plume, R., et al. 2000, ApJ, 539, L133
Plume, R., Jaffe, D. T., & Keene, J. 1994, ApJ, 425, L49
Plume, R., Jaffe, D. T., Tatematsu, K., Evans, N. J., II, & Keene, J. 1999, ApJ, 512, 768
Schröder, K., Staemmler, V., Smith, M. D., Flower, D. R., & Jacquet, R. 1991, J. Phys. B, 24, 2487
Scoville, N. Z., & Solomon, P. M. 1974, ApJ, 187, L67
Sekimoto, Y., et al. 1999, in Proceedings of Star Formation 1999, ed. T. Nakamoto (Nobeyama Radio Observatory), 86
Snell, R. L., et al. 2000, ApJ, 539, L97
Snell, R. L., Mundy, L. G., Goldsmith, P. F., Evans, N. J., II, & Erickson, N. R. 1984, ApJ, 276, 625
Stutzki, J., & Güsten, R. 1990, ApJ, 356, 513
Stutzki, J., Stacey, G. J., Genzel, R., Harris, A. I., Jaffe, D. T., & Lugten, J. B. 1988, ApJ, 332, 379
Tauber, J. A., Lis, D. C., Keene, J., Schilke, P., & Büttgenbach, T. H. 1995, A&A, 297, 567
Tielens, A. G. G. M., & Hollenbach, D. J. 1985, ApJ, 291, 722
Wang, Y., Jaffe, D. T., Evans, N. J., Hayashi, M., Tatematsu, K., & Zhou, S. 1993, ApJ, 419, 707
Wilson, C. D., Howe, J. E., & Balogh, M. L. 1999, ApJ, 517, 174